



**HAL**  
open science

# Effect of Powder Mixture Composition on the Deposition Efficiency in Cold Spay: Modelling and Experimental Validation

E. Lapushkina, A. Sova

► **To cite this version:**

E. Lapushkina, A. Sova. Effect of Powder Mixture Composition on the Deposition Efficiency in Cold Spay: Modelling and Experimental Validation. *Coatings*, 2019, 9 (12), pp.832. 10.3390/coatings9120832 . hal-03367367

**HAL Id: hal-03367367**

**<https://hal.science/hal-03367367>**

Submitted on 22 Feb 2023

**HAL** is a multi-disciplinary open access archive for the deposit and dissemination of scientific research documents, whether they are published or not. The documents may come from teaching and research institutions in France or abroad, or from public or private research centers.

L'archive ouverte pluridisciplinaire **HAL**, est destinée au dépôt et à la diffusion de documents scientifiques de niveau recherche, publiés ou non, émanant des établissements d'enseignement et de recherche français ou étrangers, des laboratoires publics ou privés.



Distributed under a Creative Commons Attribution 4.0 International License

Article

# Effect of Powder Mixture Composition on the Deposition Efficiency in Cold Spray: Modelling and Experimental Validation

E. Lapushkina <sup>1</sup> and A. Sova <sup>2,\*</sup>

<sup>1</sup> MATEIS Laboratory UMR 5510, Université de Lyon, INSA Lyon, 69621 Villeurbanne CEDEX, France; elizaveta.lapushkina@insa-lyon.fr

<sup>2</sup> LTDS Laboratory UMR 5513, National Engineering School of Saint-Etienne (ENISE), Univ Lyon, F42100 Saint-Etienne, France

\* Correspondence: alexey.sova@enise.fr

Received: 29 October 2019; Accepted: 5 December 2019; Published: 6 December 2019



**Abstract:** In this paper, a new semiempirical probability model, allowing for prediction of the composition of multimaterial cold spray coating in dependence on the initial percentage of blend components, is developed and applied. The proposed modeling approach takes into account the deposition efficiencies and the particle sizes of each component of the spraying powder blend. The experimental validation using several Cu/Cr<sub>2</sub>C<sub>3</sub>NiCr mixtures with different percentages of copper and cermet powders showed that the simulation results were in a good agreement with the experimental data. It was demonstrated that the deposition efficiency of the Cr<sub>2</sub>C<sub>3</sub>NiCr cermet powder strongly decreased when its mass percentage in the Cu/Cr<sub>2</sub>C<sub>3</sub>NiCr mixture increased from 5% to 75%. It was also shown that the dependence of the Cr<sub>2</sub>C<sub>3</sub>NiCr content in the coating on the initial percentage in the blend was nonlinear and the standard rule of mixtures was not applicable for prediction of copper–cermet coating composition.

**Keywords:** cold spray; composite; powder mixture; deposition efficiency

## 1. Introduction

In the cold spray process, particles should reach the critical value of impact energy in order to adhere to the surface. The value of the critical energy could be estimated using the equations developed by Assadi et al. [1–3], if the mechanical and thermal properties of a spray material are known. In general, the critical energy is proportional to material hardness, melting temperature, impact temperature, density, and heat capacity [4]. The required level of the critical impact energy is achieved by accelerating and heating particles with supersonic gas flow. From a technological point of view, the particle impact velocity and the temperature are controlled by adjustment of the working gas stagnation pressure, the stagnation temperature, and the nozzle geometry. Therefore, in the case of cold spray deposition of a mixture, containing several powders with significantly different mechanical and thermal properties, gas flow parameters could be appropriate for the deposition of one component of the mixture but be insufficient for the deposition of another component.

Experiments with cold spraying of different powder mixtures revealed another important phenomenon. In the case of spraying of metal blends containing powders of a soft metal and a hard metal (or ceramics) at a low gas stagnation temperature optimal for deposition of the soft metal, a composite coating containing some inclusions of hard particles embedded into the soft matrix could be formed [5–10]. At the same time, the cold spraying of the same hard powder, using the same equipment at the same low gas stagnation temperature but without addition of soft particles, does not allow building up a coating due to the zero deposition efficiency. Thus, it is possible to conclude that

the presence of the soft metal in the mixture “helps” hard particles to adhere to the surface covered by soft metal particles. This effect could be explained by the following suggestion. It is known from the previous studies that adhesion in cold spray depends on metallurgical bonding and mechanical interlocking [11]. The contribution of each mechanism strongly depends on particle/substrate properties as well as on particle impact conditions [12,13]. Strong mechanical interlocking at a coating–substrate interface is usually observed, when particles are significantly harder than the substrate. In this case, metal jetting due to the impact of incoming particles causes lips of the soft substrate material to form, which partially envelop the impacting particles [11]. Moreover, if the hardness of the impacted surface is significantly lower than the powder hardness, particles may adhere to the surface at an impact velocity lower than the critical one [14]. This effect is applied in laser-assisted cold spray, where surface softening by laser preheating allows shifting the particle adhesion mechanism from particle deformation to substrate deformation in order to decrease the particle critical velocity [15,16].

A similar effect is observed during deposition of powder blends containing soft metal and hard metal particles (Figure 1). The impact energy of soft metal particles is high enough to provide particle bonding on the substrate surface as well as on previously adhered particles of the soft or hard metal. At the same time, the impact energy of hard particles is sufficient only for bonding to the surface previously covered by the soft metal (mechanical embedding of the hard particles into the soft matrix shown in scenario 1). If hard particles reach the surface covered by previously bonded hard particles, the impact energy is not enough for bonding, and the hard particle rebounds (scenario 2). Therefore, the deposition efficiencies of “hard” and “soft” blend components are significantly different. The deposition efficiency of soft metal particles is constant, whereas the deposition efficiency of hard metal particles depends on the type of surface that hard particles reach during the impact. Obviously, scenario 1 is predominant if the spraying mixture contains a low quantity of hard metal particles. Increasing of the hard powder percentage in the mixture shifts the probability of occurrence towards to scenario 2.

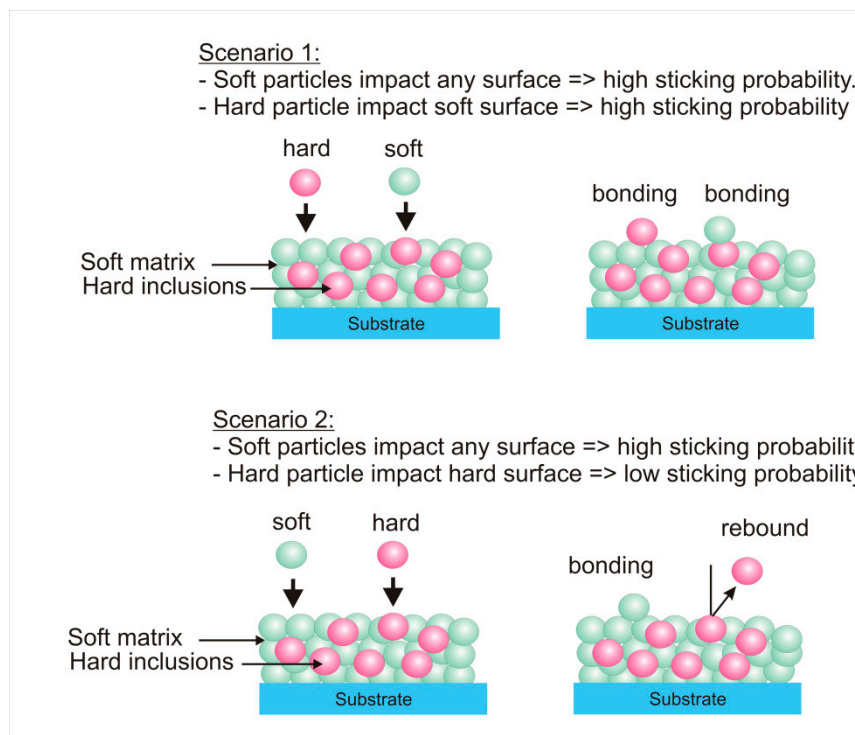


**Figure 1.** Possible particle behavior during impact in the case of cold spray of a two-component powder blend containing hard and soft components. Spray parameters are optimal for deposition of soft particles but significantly low for hard powders.

All these assumptions could be summarized as follows:

- Composition of multimaterial cold spray coating containing “soft” and “hard” particles should differ from the initial blend composition due to different deposition efficiencies of the mixture components;
- Variation of percentage of “hard” particles in the blend should change the deposition efficiency of the “hard” component as a function of its concentration in the blend;
- Prediction of coating composition by interpolation of results obtained only for one blend composition (application of the rule of mixtures) is not possible;
- From a practical point of view, it is necessary to find a method, which allows simulating the final coating composition.

In the present paper, a simple probability-based simulation model, which can evaluate the multimaterial coating composition, was proposed. Previously, this model was successfully tested for the case of cold spray deposition of a three-component metal powder mixture [17]. A similar probability-based simulation approach was applied by Klinkov and Kosarev to describe surface activation by abrasive particles during cold spraying of metal/ceramic mixtures [18].

## 2. Modeling

Relatively simple modeling of the composite coating growth could be performed if the following considerations are applied:

- A mixture contains two powders (hard and soft);
- Particles of both powders are spherical;
- Particles of hard and soft powders are well-mixed in a gas flow;
- Continuous coating is performed, and the substrate is already covered by the particles of the mixture (the first layer of the coating is formed).

These considerations allow suggesting that, during a short time interval, a total number  $dn$  of particles falls onto a unit surface. If  $C$  is the soft metal particle number concentration in a mixture, then the numbers of soft and hard metal particles falling on the surface are  $Cdn$  and  $(1 - C)dn$ , respectively. Let us also consider that the contact areas of soft and hard metal particles,  $PS_{soft}$  and  $PS_{hard}$ , respectively, are proportional to their square diameters with the same proportionality coefficient  $K$ :

$$PS_{soft} = Kd_{soft}^2$$

$$PS_{hard} = Kd_{hard}^2$$

The relative surface areas  $s_{soft}$  and  $s_{hard}$  are the surfaces already covered by adhered soft and hard metal particles, respectively. The soft particles adhere to hard and soft surfaces with probabilities of  $p_{soft-hard}$  and  $p_{soft-soft}$ , respectively. The adhesion probabilities of hard particles are  $p_{hard-soft}$  and  $p_{hard-hard}$  for soft and hard surfaces, respectively. Thus, the changing of the relative surface area covered by the soft metal per short time interval is calculated as:

$$ds_{soft} = -p_{hard-soft}(1 - C)s_{soft}PS_{hard}dn + Cp_{soft-soft}s_{hard}PS_{soft}dn \quad (1)$$

The relative surfaces occupied by hard and soft particles are related through the relationship shown in Equation (2):

$$s_{soft} + s_{hard} = 1 \quad (2)$$

If the coating formation process is stationary (the coating thickness is much higher than the particle diameter), then Equation (1) is equal to zero.

The total mass of the particles impacting the surface could be expressed as:

$$dM_p = dM_{phard} + dM_{psoft} = (1 - C)m_{hard}dn + Cm_{soft}dn \quad (3)$$

The total increase of the mass of the coating per time interval can be written as:

$$dM_c = dM_{soft} + dM_{hard} \quad (4)$$

where  $dM_{soft}$  and  $dM_{hard}$  are the masses of soft particles and hard particles, respectively, in the coating, expressed as:

$$dM_{soft} = C(p_{soft-soft}s_{soft} + p_{soft-hard}s_{hard})m_{soft}dn \quad (5)$$

$$dM_{hard} = (1 - C)(p_{hard-soft}s_{soft} + p_{hard-hard}s_{hard})m_{hard}dn \quad (6)$$

Finally, the deposition efficiency of soft and hard powders sprayed in the blend could be expressed as:

$$DE_{soft} = \frac{dM_{soft}}{dM_{psoft}} \quad (7)$$

$$DE_{hard} = \frac{dM_{hard}}{dM_{phard}} \quad (8)$$

Equations presented above allow calculating the probability of impact of hard or soft particles with the surface previously covered by adhered soft or hard particles. As a result, the deposition efficiency of the mixture components in dependence on the initial mixture composition can be calculated, if the adhesion probabilities  $p_{soft-hard}$ ,  $p_{soft-soft}$ ,  $p_{hard-soft}$ , and  $p_{hard-hard}$  are known.

In order to demonstrate how this model may be applied, the following hypothetical cases could be analyzed.

#### Case 1

This case, the ideal one, describes the situation, where particles of the hard component *B* of an *A–B* mixture stick on a surface occupied by previously adhered particles of the soft component *A* at a very high adhesion probability. At the same time, the hard component *B* is not capable to form the coating when sprayed alone due to a very low deposition efficiency. The deposition efficiency of the soft component *A* is very high and does not depend on the impacting surface. As a consequence, the following input parameters should be applied for the modeling:

- The deposition efficiency of component *A* on *A* (soft on soft) is 99%:  $p_{soft-soft} = 0.99$ ;
- The deposition efficiency of *A* and *B* (soft on hard) is 99%:  $p_{soft-hard} = 0.99$ ;
- The deposition efficiency of *B* on *A* (hard on soft) is 99%:  $p_{hard-soft} = 0.99$ ;
- The deposition efficiency of *B* on *B* (hard on hard) is 0%:  $p_{hard-hard} = 0$ ;
- The particle mean sizes as well as the densities of *A* and *B* are similar;
- The mass concentration of component *B* in the blend is varied from 1% to 99%.

Values, set for the modelling of case 1, describe the kinetics of coating formation during spraying of an “ideal” metal–ceramics powder mixture, where the pure ceramic component is not sprayable at all but ceramic particles could adhere to the soft metal matrix.

#### Case 2

In this case, typical for “soft”–“hard” metal mixtures, the hard component *B* of the mixture could be sprayed alone with a low deposition efficiency (set in the calculation at 5%), but the adhesion probability rises to 25%, if hard particles impact a surface covered by a previously adhered soft material *A*. The deposition efficiency of particles of the soft component *A* is also slightly higher than the hard one, when soft particles impact a surface covered by previously adhered soft particles:

- The deposition efficiency of component A on A (soft on soft) is 90%:  $p_{\text{soft-soft}} = 0.9$ ;
- The deposition efficiency of A and B (soft on hard) is 80%:  $p_{\text{soft-hard}} = 0.8$ ;
- The deposition efficiency of B on A (hard on soft) is 25%:  $p_{\text{hard-soft}} = 0.25$ ;
- The deposition efficiency of B on B (hard on hard) is 5%:  $p_{\text{hard-hard}} = 0.05$ ;
- The mean particle sizes as well as the densities of A and B are similar;
- The mass concentration of material B in the blend is varied from 1% to 99%.

Application of Equations (1)–(8) allows calculating the deposition efficiency of each component as well as the coating composition for both the cases. Figure 2a,b show the dependence of the deposition efficiency of the hard component B and the total blend deposition efficiency on the mixture composition. One can see from Figure 2 that the shape of the deposition efficiency curve as well as the percentage of the hard component in the coating strongly depends on the bonding probabilities of components A and B set as the model constants. However, in both the cases, the increase of the percentage of component B in the mixture decreases the deposition efficiency of material B as well as the total deposition efficiency of the mixture.

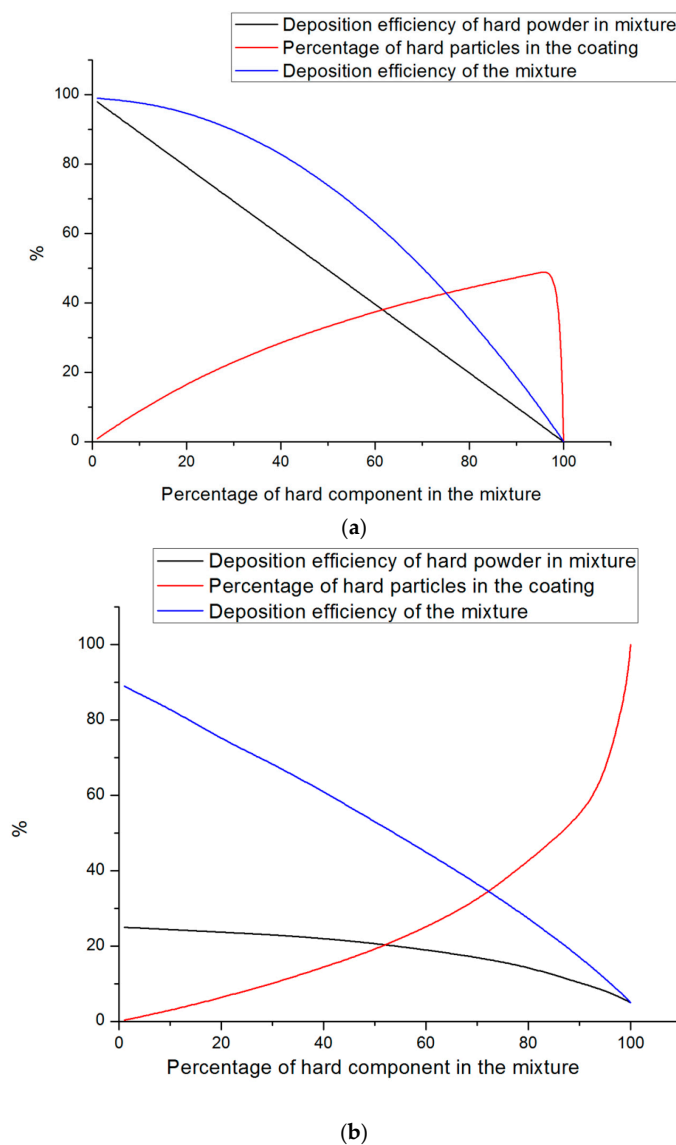


**Figure 2.** Percentage of hard particles in the coating, deposition efficiency of hard particles, and total deposition efficiency of the blend vs. percentage of the hard component in the initial blend before spraying: (a) case 1; (b) case 2.

If the concentration of the hard component in the blend before spraying is high, then the probability of impact between hard particles and the soft surface is small, and coating forms mostly, in accordance to scenario 2, with a low deposition efficiency. It is also important to note that the drop of the deposition efficiencies could be nonlinear. Figure 2 shows that, in case 1, the percentage of material *B* in the coating has a saturation limit equal to 45%. It is obvious that there is no saturation limit in case 2, because particles of the hard material *B* are able to stick to a surface covered by previously adhered hard particles with a nonzero adhesion probability. However, the deposition efficiency drastically drops down, if the percentage of material *B* in the initial blend increases.

The results presented above show that the shapes of deposition efficiency/blend composition curves strongly depend on the adhesion probabilities of the mixture components. In order to predict the final coating composition, the parameters  $p_{soft-hard}$ ,  $p_{soft-soft}$ ,  $p_{hard-soft}$ , and  $p_{hard-hard}$  must be defined.

### 3. Experimental Validation

Experimental validation of the model was performed by the cold spray deposition of two-component Cu–Cr<sub>2</sub>C<sub>3</sub>NiCr blends and followed by a comparison of experimental and theoretical results. Copper was considered as a soft component of the mixtures, whereas the Cr<sub>2</sub>C<sub>3</sub>NiCr cermet powder was used as a hard one. Gas-atomized copper and agglomerated-sintered Cr<sub>2</sub>C<sub>3</sub>NiCr (Amperit 588) powders were supplied by Sandvik Osprey (Neath, UK) and H.C. Stark (Munich, Germany), respectively. The particles size distributions measured by an ALPAGA 500 Occhio (Angleur, Belgium) optical granulomorphometer as well as the SEM images of the particles obtained by Tescan Vega3 (Kohoutovice, Czech Republic) are presented in Figure 3. One can see from Figure 3 that the mean particle sizes of both the powders were similar. The size of the largest copper particles did not exceed 45 μm, whereas the Cr<sub>2</sub>C<sub>3</sub>NiC powder contained some particles with diameters more than 50 μm. A commercial cold spray equipment CGT KINETIKS 4000 (Ampfing, Germany) with a type 40 spray nozzle was applied for coating deposition. Polished sheets produced in the 1050 aluminum alloy with a thickness of 2 mm were used as substrates. Deposition was performed with the spraying parameters listed in Table 1. In order to minimize the influence of the substrate on the kinetics of the coating formation process, thick coatings (thickness: more than 3 mm) were deposited and analyzed.

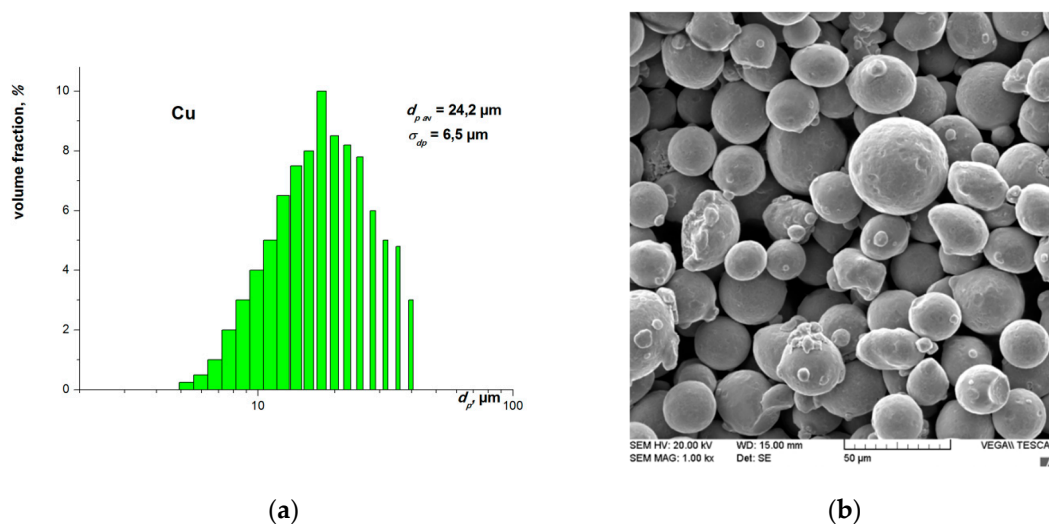
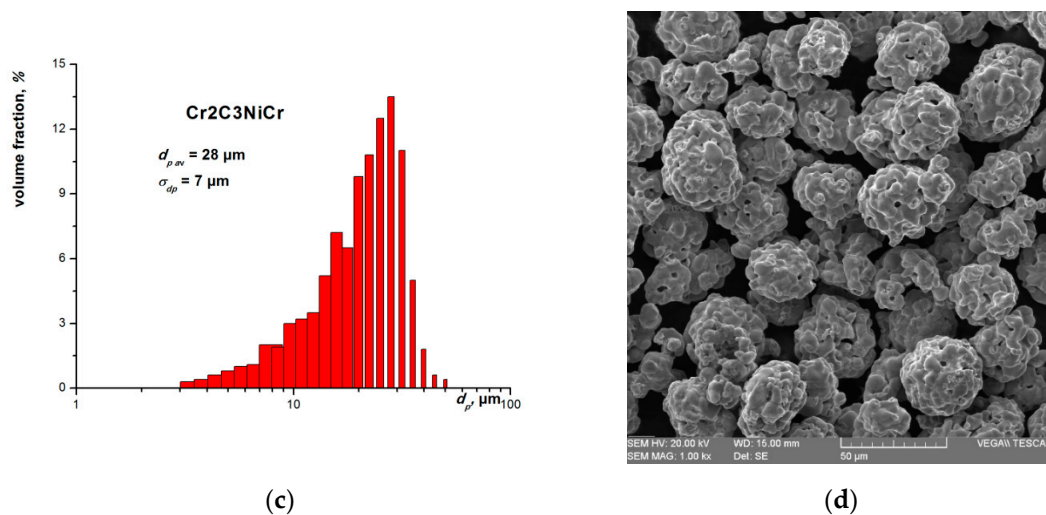


Figure 3. Cont.



**Figure 3.** Particle size distribution (a) and SEM image (b) of the Cu powder used in the experiments. Particle size distribution (c) and SEM image (d) of the Cr<sub>2</sub>C<sub>3</sub>NiCr powder used in the experiments.

**Table 1.** Spraying parameters.

Gas Type	Gas Pressure $p_0$ (bar)	Gas Stagnation Temperature $T_0$ (°C)	Nozzle Traverse Speed (mm/s)	Track Overlapping (mm)	Number of Layers	Spraying Distance (mm)
Nitrogen	35	350 °C 450 °C	10	3	2–10	40

Coating composition was determined by cross-sectional SEM image analysis. The blend compositions used in the experiments are listed in Table 2.

**Table 2.** Powder mixtures used in the experiments.

	Cu (wt %)	Cr <sub>2</sub> C <sub>3</sub> NiCr (wt %)
Blend 1	100	0
Blend 2	0	100
Blend 3	95	5
Blend 4	90	10
Blend 5	75	25
Blend 6	50	50
Blend 7	25	75

The total mixture deposition efficiency was measured in the following way. Firstly, the powder feed rate was estimated by weighing the powder injected from the feeder into a closed volume after 30 and 60 s time intervals. Secondly, the deposition efficiency was calculated using the following relationship:

$$\text{Deposition efficiency} = \frac{M}{R \times t} \quad (9)$$

where  $M$  is the coating mass,  $R$  is the powder feed rate, and  $t$  is the spraying time. With Equation (9) and the results of the coating composition analysis, the total deposition efficiency, as well as the deposition efficiencies of copper (soft component) and cermet (hard component) for each blend, can be calculated.



The first series of experiments were carried out in order to determine the constant probabilities  $p_{\text{soft-hard}}$ ,  $p_{\text{soft-soft}}$ ,  $p_{\text{hard-soft}}$ , and  $p_{\text{hard-hard}}$  necessary for simulation. It was considered that, in the case of spraying of pure copper or pure cermet powders, particles always impacted the surface covered by previously adhered particles of the same material, and the measured total deposition efficiency of the powder was equal to the adhesion probability. Therefore, the values of the deposition efficiencies measured for the pure Cu and Cr<sub>2</sub>C<sub>3</sub>NiCr powders (blends 1 and 2) were further used in the simulation as the adhesion probabilities  $p_{\text{soft-soft}}$  and  $p_{\text{hard-hard}}$ , respectively. In order to determine the probability  $p_{\text{hard-soft}}$ , the tests with spraying of the two-component blend with a low percentage (5 wt %) of the Cr<sub>2</sub>C<sub>3</sub>NiCr powder were performed (blend 3). It was considered that, due to the low concentration of the Cr<sub>2</sub>C<sub>3</sub>NiCr particles in the blend, the number of impacts between upcoming hard particles and previously adhered hard particles on the coating surface was negligible, and the impacts between cermet particles and a soft surface formed by copper particles were predominant. Thus, knowing the concentration of the Cr<sub>2</sub>C<sub>3</sub>NiCr particles in the coating, the initial composition of the blend, and the total blend deposition efficiency, the probability  $p_{\text{hard-soft}}$  could be calculated. At the same time it was difficult to measure the adhesion probability of Cu particles on the hard Cr<sub>2</sub>C<sub>3</sub>NiCr surface due to a very low total deposition efficiency in the case of spraying of cermet-rich blends. Therefore, it was assumed that the probability  $p_{\text{soft-hard}}$  was approximately the same as  $p_{\text{soft-soft}}$ . Experimental values of the probabilities  $p_{\text{soft-hard}}$ ,  $p_{\text{soft-soft}}$ ,  $p_{\text{hard-soft}}$ , and  $p_{\text{hard-hard}}$  obtained for blends 1–3 were further used as the model constants. After that, the theoretical coating composition for all possible blend percentages was simulated using Equations (1)–(8) and compared with the experimental results obtained for blends 4–7.

Examples of the composite coatings cross-sections are presented in Figure 4. The microstructure of the obtained deposits was typical for cold spray composites. The hard particles of Cr<sub>2</sub>C<sub>3</sub>NiCr were uniformly distributed in the soft matrix of copper as the separated inclusions. The experimentally determined values of  $p_{\text{soft-soft}}$ ,  $p_{\text{hard-soft}}$ , and  $p_{\text{hard-hard}}$  indicated as  $p_{\text{Cu-Cu}}$ ,  $p_{\text{cermet-Cu}}$ , and  $p_{\text{cermet-cermet}}$  were reported in Figure 5. Figure 5 shows that the adhesion probability of copper on copper is equal to ~50% and ~60% for the gas stagnation temperature  $T_0$  of 350 and 450 °C, respectively. The same values of adhesion probability were set for  $p_{\text{Cu-cermet}}$ . The deposition efficiency of the pure Cr<sub>2</sub>C<sub>3</sub>NiCr powder was close to zero for both the gas stagnation temperatures. However, in the case of spraying of the Cu/5% Cr<sub>2</sub>C<sub>3</sub>NiCr mixture, the particles of Cr<sub>2</sub>C<sub>3</sub>NiCr powder adhered to the copper surface with adhesion probabilities of ~14% ( $T_0 = 450$  °C) and ~8% ( $T_0 = 350$  °C). It is possible to suggest that the rise of the gas stagnation temperature increases the cermet particle impact velocity. Impact at a higher velocity intensifies the deformation of copper matrix and increases the adhesion probability of Cr<sub>2</sub>C<sub>3</sub>NiCr particles on the copper matrix.

In Figures 6 and 7, a comparison between the results obtained by numerical simulation and experimental measurements are presented. The theoretical curve fits well with the experimental points that confirms the reliability of the model. It is important to note that the deposition efficiency of the Cr<sub>2</sub>C<sub>3</sub>NiCr powder dropped nonlinearly, if the percentage of copper in the mixture decreased, which was confirmed by experimental measurements. The maximum possible concentration of Cr<sub>2</sub>C<sub>3</sub>NiCr in the coating obtained in the experiments was 26% for the blend containing 75% of cermet before spraying, which correlated well with the simulation results. The simulation also showed that the maximum possible concentration of cermet in coating cannot be higher than 45% for  $T_0 = 450$  °C and 32% for  $T_0 = 350$  °C.

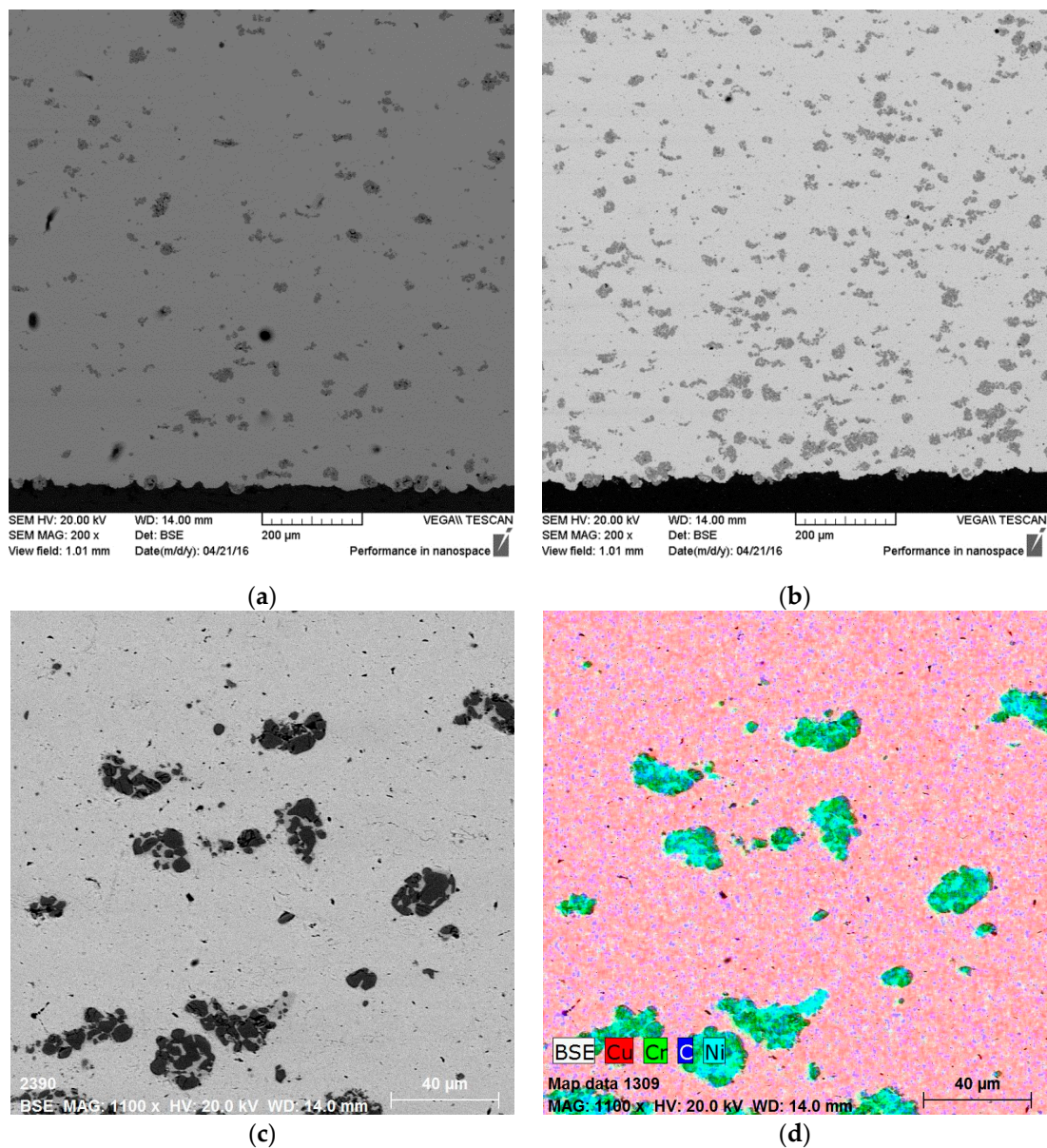


**Figure 4.** SEM images of coating cross-section deposited using different blends: (a) Cu/10% Cr<sub>2</sub>C<sub>3</sub>NiCr mixture, (b) Cu/50% Cr<sub>2</sub>C<sub>3</sub>NiCr mixture, (c) Cu/25% Cr<sub>2</sub>C<sub>3</sub>NiCr mixture, (d) – Cu/25% Cr<sub>2</sub>C<sub>3</sub>NiCr mixture with EDX analysis. All samples were sprayed at  $T_0 = 450\text{ }^\circ\text{C}$ .

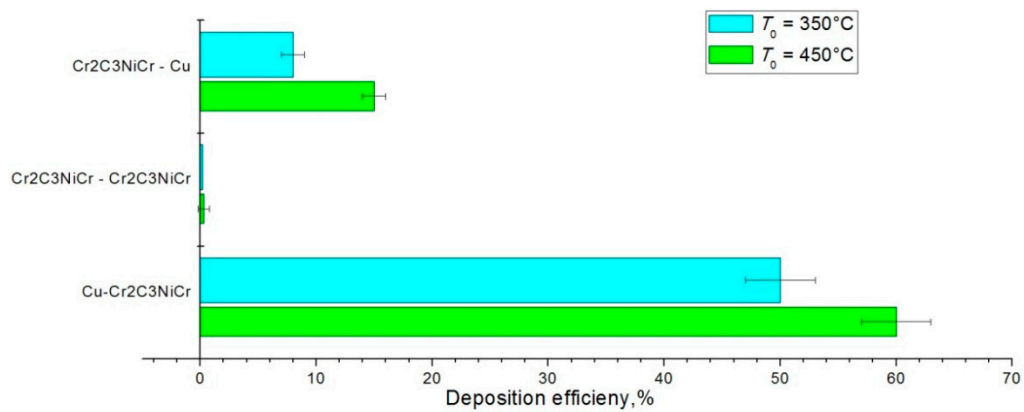


**Figure 5.** Adhesion probabilities of the copper and Cr<sub>2</sub>C<sub>3</sub>NiCr particles.

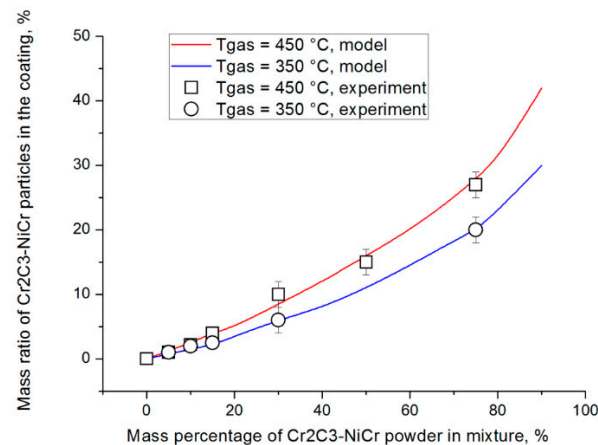


Figure 6. Percentage of the hard component in the coating vs. blend initial composition before spraying.

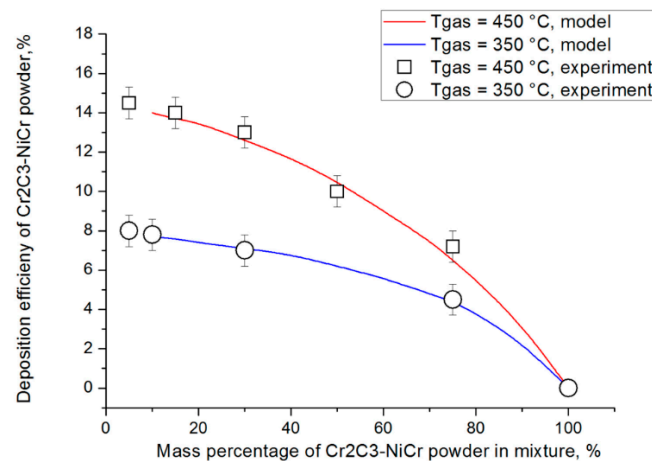


Figure 7. Deposition efficiency of the hard blend component vs. initial blend composition.

#### 4. Discussion

The obtained experimental and numerical results showed that the composition of multimaterial cold spray coating could be predicted using simple probability-based modeling. It was also demonstrated that the shape of the deposition efficiency curve strongly depended on the bonding probability values set as the model constants. In this study, these values were found by experimental measurements of the deposition efficiencies of blends 1–3. However, this method does not allow determining of probability  $p_{soft-hard}$  with high precision. A rough approximation of  $p_{soft-soft} = p_{soft-hard}$  applied in this study allowed obtaining the reliable modeling results in given cases with the deposition of a Cu–Cr<sub>2</sub>C<sub>3</sub>NiCr mixture, but it could be inapplicable for mixtures of other powder materials, where adhesion probabilities  $p_{soft-soft}$  and  $p_{soft-hard}$  could be significantly different. One of the possible ways of prediction of particle adhesion probability is the splat test [19,20]. An important work devoted to the application of the splat test method for determining of particle bonding probability in the case of deposition of a 316 L–Fe powder mixture was done and published by Chu et al. [21]. This approach could significantly increase the modeling accuracy, but at the same time a large amount of expensive experimental measurements are required.

Another important question is the influence of substrate on the kinetics of composite coating growth. In the current model, it is assumed that the coating thickness is high (no influence of substrate), and the coating formation process is stationary. However, in general cases, the adhesion probabilities of the first generation of particles interacting with the substrate material  $p_{soft-substrate}$  and  $p_{hard-substrate}$

could significantly differ from  $p_{\text{soft-soft}}$ ,  $p_{\text{hard-soft}}$ ,  $p_{\text{hard-hard}}$ , and  $p_{\text{soft-hard}}$ . As a consequence, the gradient of composition could be observed at the near-substrate coating layer.

The influence of particle superposition during impact should be also taken into account. It is clear that one part of hard particles could impact the soft surface whereas the other part could impact the hard one. In this case, the bonding probability  $p_{\text{hard-soft}}$  must be adjusted. This effect should be especially important in the case of deposition of metal–ceramic mixtures with significantly different particle size distributions.

Finally, the effect of surface activation previously discussed by Irissou et al. [9], Klinkov and Kosarev [18], Shkodkin et al. [22], and Grigoriev et al. [23] should be taken into account. In particular, it is known that the deposition efficiency of a metal powder mixed with hard particles could be higher than in the case, when the same metal powder is sprayed alone [22]. It is suggested that the high-velocity impact of hard ceramic particles “cleans”, in some manner, the coating surface covered by previously adhered metal particles and increases its chemical/metallurgical activity. In other words, ceramic particle does not stick to the soft matrix due to a low  $p_{\text{hard-soft}}$  probability value but changes the material properties of the soft matrix in the impact zone. As a consequence, the bonding probability between upcoming metal particles and the activated surface  $p_{\text{soft-soft\_activated}}$  becomes higher than  $p_{\text{soft-soft}}$  established for the nonactivated soft surface. It is interesting to note that a similar activation effect obtained for a metal–metal powder mixture was reported in the work of Chu et al. [21]. In particular, they noticed that addition of a small amount of the “harder” 316 L powder to a 316 L–iron mixture increased the deposition efficiency of the “softer” Fe component from 38% to 55%. Evidently, that correct determination of  $p_{\text{soft-soft\_activated}}$  is a complex task, and further researches should be conducted in order to develop a methodology allowing taking into account this activation effect.

## 5. Conclusions

The developed semiempirical probability-based approach allows simulating the kinetics of a composite coating formation process in the case of cold spray deposition of powder mixtures. The obtained results showed that the deposition efficiency of the hard component in the blend strongly depended on the initial share of the hard component in the mixture. A good correlation between the experimental results and the modeling confirmed the reliability of the considerations placed in the model base. Further model development should be performed in order to take into account the influence of a substrate, particle superposition, and activation effects on the bonding probability and the resulting coating composition.

**Author Contributions:** Conceptualization, A.S.; methodology, A.S. and E.L.; validation, E.L.; formal analysis E.L. and A.S.; writing—original draft preparation, A.S.; writing—review and editing, A.S.

**Funding:** This research received no external funding.

**Conflicts of Interest:** The authors declare no conflict of interest.

## Nomenclature

$s_{\text{soft}}$	Relative area of a surface covered by a soft metal
$s_{\text{hard}}$	Relative area of a surface covered by a hard metal
$PS_{\text{soft}}$	Contact surface area of soft metal particles
$PS_{\text{hard}}$	Contact surface area of hard metal particles
$p_{\text{soft-soft}}$	Probability of soft metal particles adhering to a surface covered by soft metal particles
$p_{\text{soft-hard}}$	Probability of soft metal particles adhering to a surface covered by hard metal particles
$p_{\text{hard-soft}}$	Probability of hard metal particles adhering to a surface covered by soft metal particles
$p_{\text{hard-hard}}$	Probability of hard metal particles adhering to a surface covered by hard metal particles
$M_{\text{soft}}$	Mass of soft particles in a coating
$M_{\text{psoft}}$	Total mass of soft particles impacting a surface
$M_{\text{hard}}$	Mass of hard particles in a coating
$M_{\text{phard}}$	Total mass of hard particles impacting a surface

$M_p$	Total mass of all particles impacting a surface
$DE_{soft}$	Deposition efficiency of a soft metal
$DE_{hard}$	Deposition efficiency of a hard metal
$C$	Number concentration of soft particles in a spray mixture
$n$	Number of particles falling onto a surface

## References

1. Assadi, H.; Gartner, F.; Stoltenhoff, T.; Kreye, H. Bonding mechanism in cold gas spraying. *Acta Mater.* **2003**, *51*, 4379–4394. [[CrossRef](#)]
2. Schmidt, T.; Assadi, H.; Gartner, F.; Richter, H.; Stoltenhoff, T.; Kreye, H.; Klassen, T. From particle acceleration to impact and bonding in cold spraying. *J. Therm. Spray Technol.* **2009**, *18*, 794–808. [[CrossRef](#)]
3. Assadi, H.; Schmidt, T.; Richter, H.; Kliemann, J.O.; Binder, K.; Gartner, F. On parameter selection in cold spraying. *J. Therm. Spray Technol.* **2011**, *20*, 1161–1176. [[CrossRef](#)]
4. Assadi, H.; Kreye, H.; Gartner, F.; Klassen, T. Cold spraying—A materials perspective. *Acta Mater.* **2016**, *116*, 382–407. [[CrossRef](#)]
5. Klinkov, S.V.; Kosarev, V.F.; Sova, A.A.; Smurov, I. Deposition of multicomponent coatings by cold spray. *Surf. Coat. Technol.* **2008**, *202*, 5858–5862. [[CrossRef](#)]
6. Vilafuerte, J. *Modern Cold Spray: Theory Process and Applications*; Springer International Publishing: Cham, Switzerland, 2015.
7. Koivuluoto, H.; Vuoristo, P. Effect of powder type and composition on structure and mechanical properties of Cu+Al<sub>2</sub>O<sub>3</sub> coatings prepared by using low-pressure cold spray process. *J. Therm. Spray Technol.* **2010**, *19*, 1081–1092. [[CrossRef](#)]
8. Spencer, K.; Fabijanic, D.M.; Zhang, X.M. The influence of Al<sub>2</sub>O<sub>3</sub> reinforcement on the properties of stainless steel cold spray coatings. *Surf. Coat. Technol.* **2012**, *206*, 3275–3282. [[CrossRef](#)]
9. Irissou, E.; Legoux, J.G.; Arsenault, B.; Moreau, C. Investigation of Al-Al<sub>2</sub>O<sub>3</sub> cold spray coating formation and properties. *J. Therm. Spray Technol.* **2007**, *16*, 661–668. [[CrossRef](#)]
10. Guo, X.; Zhang, G.; Li, W.; Gao, Y.; Liao, H.; Coddet, C. Investigation of the microstructure and tribological behavior of cold-sprayed tin-bronze-based composite coatings. *Appl. Surf. Sci.* **2009**, *255*, 3822–3828. [[CrossRef](#)]
11. Hussain, T.; McCartney, D.G.; Shipway, P.H.; Zhang, D. Bonding mechanisms in cold spraying: The contributions of metallurgical and mechanical components. *J. Therm. Spray Technol.* **2009**, *18*, 364–379. [[CrossRef](#)]
12. Huang, R.; Ma, W.; Fukanuma, H. Development of ultra-strong adhesive strength coatings using cold spray. *Surf. Coat. Technol.* **2014**, *258*, 832–841. [[CrossRef](#)]
13. Drehmann, R.; Grund, T.; Lampke, T.; Wielage, B.; Manyoats, K.; Schucknecht, T.; Rafaja, D. Interface characterization and bonding mechanisms of cold gas-sprayed Al coatings on ceramic substrates. *J. Therm. Spray Technol.* **2014**, *24*, 92–99. [[CrossRef](#)]
14. Bray, M.; Cockburn, A.; O'Neill, W. The laser assisted cold spray process and deposit characterization. *Surf. Coat. Technol.* **2009**, *203*, 2851–2857. [[CrossRef](#)]
15. Lupoi, R.; Sparkes, M.; Cockburn, A.; O'Neill, W. High speed titanium coatings by supersonic laser deposition. *Mater. Lett.* **2011**, *65*, 3205–3207. [[CrossRef](#)]
16. Fang, L.U.O.; Lupoi, R.; Cockburn, A.; Sparkes, M.; O'Neill, W.; Yao, J.H. Characteristics of Stellite 6 deposited by supersonic laser deposition under optimized parameters. *J. Iron Steel Res. Int.* **2013**, *20*, 52–57.
17. Sova, A.; Maestracci, R.; Jeandin, M.; Bertrand, P.; Smurov, I. Kinetics of composite coating formation process in cold spray: Modelling and experimental validation. *Surf. Coat. Technol.* **2017**, *318*, 309–314. [[CrossRef](#)]
18. Klinkov, S.; Kosarev, V. Cold spraying activation using an abrasive admixture. *J. Therm. Spray Technol.* **2012**, *21*, 1046–1053. [[CrossRef](#)]
19. Xiong, Y.; Bae, G.; Xiong, X.; Lee, C. The effects of successive impacts and coldwelds on the deposition onset of cold spray coatings. *J. Therm. Spray Technol.* **2009**, *19*, 575–585. [[CrossRef](#)]
20. Wu, J.; Fang, H.; Yoon, S.; Kim, H.; Lee, C. The rebound phenomenon in kinetic spraying deposition. *Scr. Mater.* **2006**, *54*, 665–669. [[CrossRef](#)]

21. Chu, X.; Che, H.; Vo, P.; Chakrabarty, R.; Sun, B.; Song, J.; Yue, S. Understanding the cold spray deposition efficiencies of 316L/Fe mixed powders by performing splat tests onto as-polished coatings. *Surf. Coat. Technol.* **2017**, *324*, 353–360. [[CrossRef](#)]
22. Shkodkin, A.; Kashirin, A.; Klyuev, O.; Buzdygar, T. Metal particle deposition stimulation by surface abrasive treatment in gas dynamic spraying. *J. Therm. Spray Technol.* **2006**, *15*, 382–385. [[CrossRef](#)]
23. Grigoriev, S.; Okunkova, A.; Sova, A.; Bertrand, P.; Smurov, I. Cold spraying: From process fundamentals towards advanced applications. *Surf. Coat. Technol.* **2015**, *268*, 77–84. [[CrossRef](#)]



© 2019 by the authors. Licensee MDPI, Basel, Switzerland. This article is an open access article distributed under the terms and conditions of the Creative Commons Attribution (CC BY) license (<http://creativecommons.org/licenses/by/4.0/>).